Indian Journal of Engineering & Materials Sciences
Vol. 28, June 2021, pp. 234-239

Establish time-temperature-transformation diagram based on dilatometry results and microstructural evolutions in an AISI 1010 steel

Yashwant Mehta[a], Sunil Kumar Rajput[b*] & Sanjeev Kumar[c]

[a]Department of Metallurgical and Materials Engineering, National Institute of Technology, Srinagar 190 006, India

[b]Department of Mechanical Engineering, Bundelkhand Institute of Engineering and Technology, Jhansi 284 128, India

[c]Institute of Materials Science and Technology, TU Wien, Getreidemarkt 9, 1040 Vienna, Austria

Received: 31 January 2021; Accepted: 06 June 2021

A time-temperature-transformation (TTT) diagram has been constructed using dilation results. The phase transformations have been confirmed through microstructural changes of AISI 1010 steel. The strength of this steel has been improved for various applications using heat treatments. Experiments for a series of steel samples have been conducted between 310-730°C isothermal temperature range using a thermo-mechanical simulator Gleeble®3800. The austenitised microstructure of the steel has been transformed into a combination of ferrite, pearlite, widmanstätten ferrite, massive ferrite, upper and lower bainite, and martensite, etc., when held at different isothermal temperatures. Ferrite along with pearlite have been observed at higher isothermal temperatures while bainite with martensite have been observed at lower isothermal temperatures. Two C-curves have been observed in pearlite and bainite transformation regions.

Keywords: Isothermal transformation, Microstructure, Plain carbon steel, Thermo-mechanical simulation, Time-temperature-transformation (TTT) diagram

1 Introduction

Plain carbon steels such as AISI 1010 have been found to possess good formability and ductility[1]. AISI 1010 has been considered as an ideal steel for the automobile industry, where it has been frequently used for auto bodies, fenders, and smaller parts including cold headed fasteners, bolt, pans, and transmission covers, etc.[2-6]. Cast steel has been found to be unsuitable for all those applications where the requirements of mechanical properties are different from those possessed by it. The heat treatment process has played an important role in changing the microstructure which provides unique properties for the product. For a better understanding of heat treatments of steel, a time-temperature-transformation (TTT) diagram has been a requirement. Using the TTT diagram the phase transformation sequence for microstructures has been estimated in terms of temperature and time. The TTT diagram has been developed by Davenport and Bain in 1930 and has been a breakthrough in understanding the kinetics of bulk phase transformations[7]. Therefore, an accurate calculation of the TTT diagram has been considered essential for promoting the development of steel. Many researchers have been reporting their work on isothermal temperature transformations for different grades of steel[8-19]. These researchers have concentrated on research work in some specific regions such as pearlite, bainite, and martensite which have been found suitable according to the industrial and daily use applications. Kumar *et al.*[15,20] have reported their work in a wide range of isothermal temperatures for high strength steel and micro-alloyed steel, but still no research work has been found related to the isothermal transformation temperature in the open literature for plain low carbon steel while the demand for such steels have been higher as discussed above. The purpose of this study has been to fill this gap and provide possible heat treatment processes for a wide range of isothermal temperatures. All isothermal heat treatments have been performed using thermo-mechanical simulator Gleeble®3800 which provides a high accuracy during the collection of phase transformation data. Dilation results and microstructural evolution have been used to construct the time temperature-transformation diagram for a wide range of isothermal temperatures.

*Corresponding author
(E-mail: rajput_skumar@rediffmail.com, rajputskmt@gmail.com)

2 Materials and Methods

Commercial grade AISI 1010 steel was used for the present work. Its chemical composition is displayed in Table 1. For the experiments intended to investigate the isothermal transformations, a special type of geometry (Fig. 1) was machined for the desired cooling rate according to ASTM standards which was deemed necessary for working between solutionizing temperature to isothermal temperature. Care was taken to avoid any kind of transformation of austenite to product phase and another purpose was to freeze the microstructure through faster cooling after complete transformation of austenite to product phase at a specific isothermal temperature. A K type (chromel-alumel) thermocouple was placed at the centre of the sample for controlled heating and recording the actual temperature cycles.

All isothermal tests were performed using the Thermo-mechanical simulator Gleeble®3800. The program was written for the iso-thermal cycles in Tabular format on Quicksim software, where the samples were heated at 10°C/s to a peak temperature of 1000°C and held at that temperature for 5 minutes. Later, the temperature of the samples was lowered at a rate of 175°C/s down to 10 distinct isothermal temperatures (IT). These IT temperatures were 730, 670, 610, 550, 490, 430, 370, and 310°C. The samples were held for 100s to 3700s at these temperatures till the phase transformation was complete. The samples were water quenched to freeze the microstructure after the completion of the isothermal transformation. A schematic thermal profile of an isothermal transformation temperature cycle at 550°C is displayed in Fig. 2. The transformation times were elongated for the confirmation of 100% phase transformation.

Table 1 — Chemical composition of the steel-AISI 1010

Element	C	Mn	Si	S	P	Fe
Wt. %	0.09	0.32	0.073	0.012	0.019	Balance

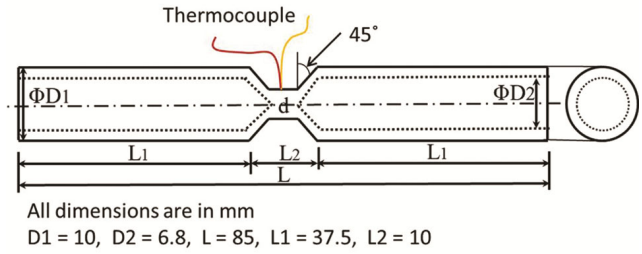

Fig. 1 — Specimen used in the ITT process[15].

For the microstructural characterization, all simulated samples were cross-sectionally sliced at the central position where the thermocouple and linear variable differential transducer (LVDT) dilatometer was placed during isothermal transformation tests. One of the two portions obtained was cold mounted in resin in order to facilitate handling of the specimen while grinding and polishing. Progressively fine silicon carbide emery papers (320, 800, 1200, and 1500 grit respectively) were used to grind the samples. The orientation of the sample was carefully changed by right angles while changing the emery papers. Once a flat surface was obtained it was subjected to polishing on a wet velvet cloth using alumina powder (1μm) to a mirror finish. The sample was rotated periodically in order to avoid the formation of comet tails. Subsequently, the sample was etched using 2% Nital (98% Methyl Alcohol and 2% Nitric Acid) in order to reveal the microstructure. The revealed microstructure was recorded after careful examination using an optical microscope. The ImageJ software facility was used to calculate the grain size and fraction of phase.

3 Results and Discussion

The isothermal transformation tests were performed on the steel samples which resulted in the formation of microstructures. Further, dilation curves were obtained. The time-temperature transformation diagram was drawn based on these dilation curves and isothermal microstructures. The initial status of the base steel was also studied and reported.

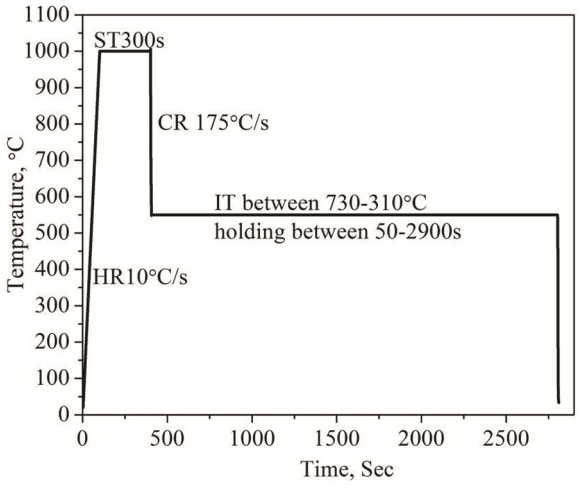

Fig. 2 — Temperature profile versus time for isothermal temperature 550°C of low carbon steel.

3.1 Microstructural characterization

As-received microstructure of AISI 1010 steel primarily consisted of ferrite (F) and pearlite (P) that can be seen in Fig. 3. Most of the pearlite phase was formed along the ferrite Grain Boundaries (GB) and at the junction points[1]. The fraction of ferrite and pearlite of the base steel was measured as 84% and 16%, respectively.

Figures 4 and 5 show the microstructure of isothermal transformed products of AISI 1010 steel after different IT heat treatments. At IT 730°C, the microstructure consisted of ferrite, pearlite, and new ferrite with carbides (Fig. 4(a)). The ferrite grains are refined as compared to the base steel microstructure. This could be attributed to the hold at lower IT than that required for austenitized condition. With a decrease in the isothermal temperature (IT 670°C), other phases are evolved such as ferrite, massive ferrite, and few nuclei of Widmanstätten Ferrite (WF). Here, primary WF either directly grows from the austenite grain surfaces and secondary WF evolves from allotriomorphic ferrite[15]. Besides, most of the pearlite phase was completely dispersed into massive ferrite and some soft pearlite was found along the ferrite grain boundaries (Fig. 4(b)). At IT 610°C, most of the ferrite phase was observed along the grain boundary in the form of pro-eutectoid ferrite while the fraction of WF was increased due to the increase in driving force. Furthermore, soft pearlite was also completely dispersed in massive ferrite and WF (Fig. 4(c)). While Fig. 4(d) displayed both ferrite and massive ferrite, presence of massive ferrite grains was found to have decreased along the grain boundaries and at the centre, respectively with decreasing IT temperature (IT 550°C). New bainite phase evolved at this temperature, and massive ferrite was replaced by this new

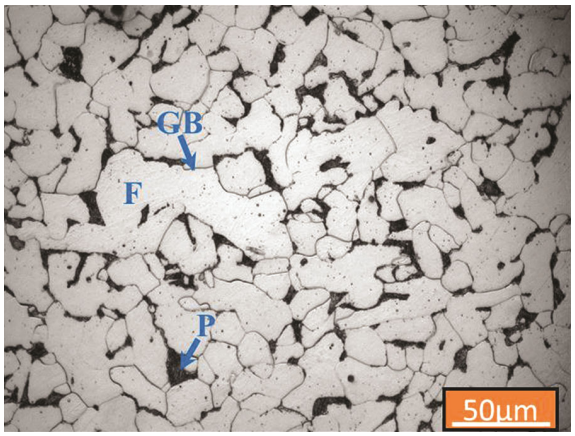

Fig. 3 — As-received microstructure of AISI 1010 steel (F = ferrite, P = pearlite, GB = grain boundary).

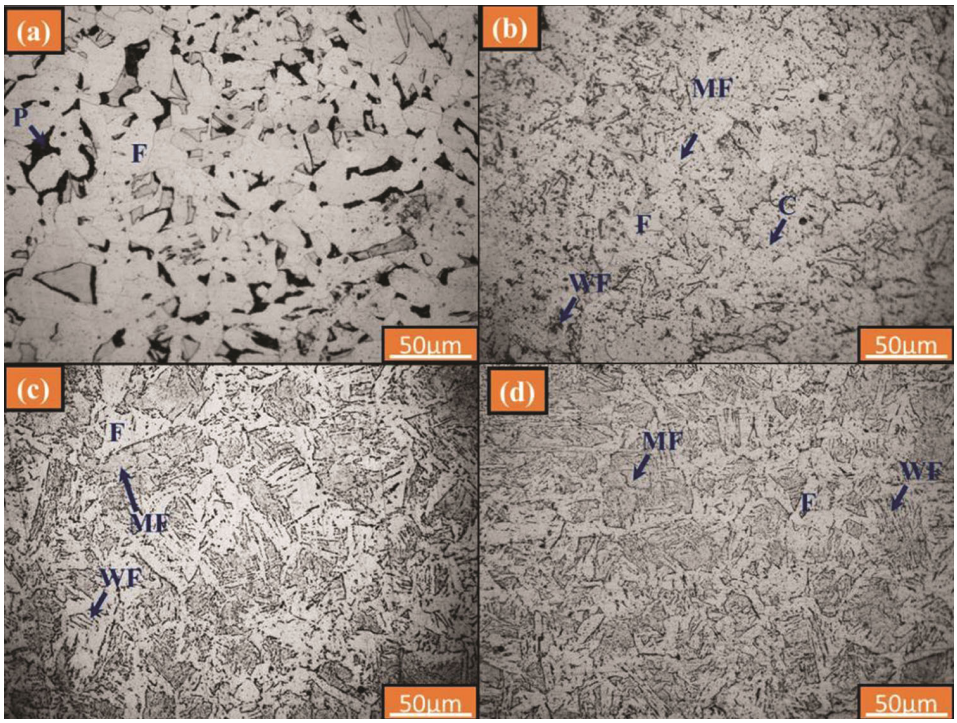

Fig. 4 — The microstructure of isothermal transformed products of low carbon steel after the isothermal temperature at (a) 730 °C, (b) 670 °C, (c) 610 °C, and (d) 550 °C (where phases are, F: ferrite; P: pearlite; MF: Massive ferrite, C: carbides; and WF: widmanstätten ferrite, etc.).

bainite structure due to suitable temperature and other conditions as well. The width of pro-eutectoid ferrite decreased with temperature. These bainite structures had formed and grown by displacive mechanism[20].

Figure 5(a) shows that the upper bainite (bainitic ferrite) fraction was found to be higher, with increase in the growth of WF due to the high amount of strain caused by higher driving force and lower IT of 470°C. The fraction of massive ferrite was continuously decreased and replaced by lower bainite with lowering of temperature. While ferrite fraction was observed in a discontinuous manner with decreasing temperature (Fig. 5(b)). Below IT of 430°C, most of the massive ferrite and upper bainite phases were transformed into lower bainite and martensite trapped most of the carbon due to the displacive mechanism which occured at the behest of a very strong driving force (Fig. 5 (c-d)). Martensite was formed due to the rapid cooling of the austenite form of iron so that carbon atoms did not have sufficient time to diffuse out the crystal structure. Further, the nucleation of martensite was diffusionless. One more observation was that the finer plates of WF were obtained with decreasing temperature (Fig. 5).

3.2 Overall transformation results

The critical temperatures were measured from the plot of dilation vs temperature, where humps were revealed during heating and cooling due to the change in packing density of the crystal structure as can be seen in Fig. 6. This hump was observed in reference to expansion and contraction during thermal cycles. During heating, the crystal structure was changed from body-centered cubic (bcc) to face-

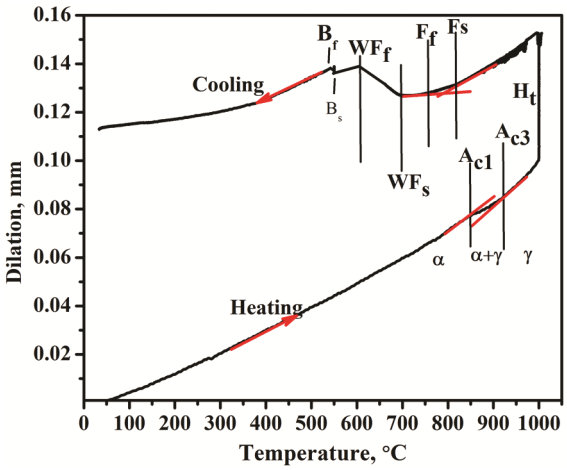

Fig. 6 — Dilation versus temperature plot during heating and cooling of AISI 1010 steel at isothermal temperature 550°C.

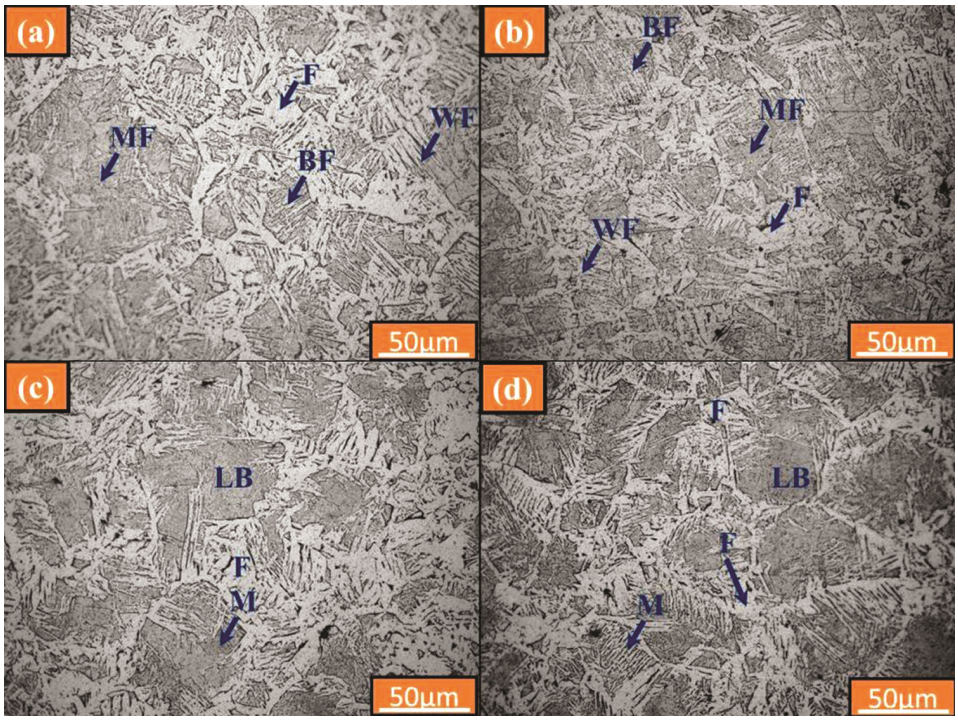

Fig. 5 — The microstructure of isothermal transformed products of low carbon steel after the isothermal temperature at (a) 490 °C, (b) 430 °C, (c) 370 °C, and (d) 310 °C (where phases are, F: ferrite; M: martensite; MF: Massive ferrite, BF: bainitic ferrite; UB: upper bainite; LB: lower bainite; and WF: widmanstätten ferrite, etc.).

centered cubic (fcc) structure which means that the ferrite phase was converted into austenite phase while fcc phase converted into bcc and bct structure and other phases as well, during the cooling cycle. Figure 6 shows during cooling that the austenite phase changed into product phases as F, WF, and Bainite structure, etc. The upper critical (A_{c3}) and lower critical (A_{c1}) temperatures obtained were 919°C, and 840°C, respectively (Fig. 6). The region between inter-critical temperatures consisted of ferrite and austenite structure. During isothermal holding, the expansion could be seen in the plot due to the continuous growth in grains until the cooling started. Three different humps were seen in the plot which represents the ferrite, WF, and bainite transformation.

Figure 7 shows the dilation vs time plot for an isothermal temperature of 550°C by which it was observed that the dilation indicating transformation started at about 403 seconds and the incubation period was approximately 0.4s. Therefore, there was 0% transformation upto 1.6 seconds and the transformation was completed at about 297s. The complete transformation has been observed after 1000s beyond which no more change in dilation was observed (Fig. 7). Other fractions such as 25%, 50%, and 75% transformation times were calculated based on the proportion of dilation which provided the corresponding temperature readings that helped in deciding the relationship for the time-temperature-transformation. Thus, the same calculation steps were followed for other isothermal temperatures.

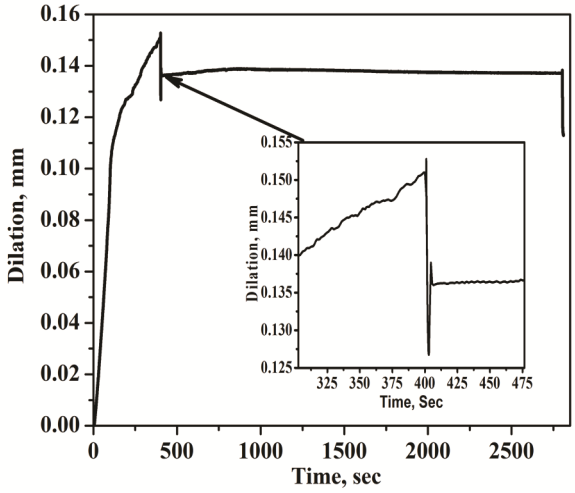

Fig. 7 — Experimental dilation versus temperature plot at an isothermal temperature of 550°C.

3.3 Construction of the time-temperature-transformation (TTT) diagram

The time-temperature-transformation diagram was constructed based on dilation curves and microstructural evolution and can be seen in Fig. 8. On the basis of microstructural evolution, the diagram was categorized into four regions. It was worthy to note that the incubation time was the longest (1.2s) for the temperature of 730°C where ferrite and pearlite were formed in higher amounts. In this incubation period, no austenite phase was transformed into any product phases. It was not possible due to the supercooling @175°C/s which would not allow any kind of transformation, but after the incubation time, transformation could be understood by the change in dilation (Fig. 8). The austenite phase stability decreased with decreasing isothermal temperature upto 610°C, and later it started to increase. The isothermal transformation diagram showed that the C curve displayed the lowest stability of austenite at 610°C. Above and below that temperature, austenite was slightly more stable. But the stability was for a time period of less than 0.5s. Half of the austenite transformed between 1 and 50s. The transformation was completed between 800 to 3000 seconds according to the temperature. Two C curves were visible at the full transformation side in which one was above the bainite transformation and the other was below that. It was also worthy to be noticed that the nose of the upper C-curve was leftward as compared to the second C-curve, in both cases of starting and ending of transformation. Furthermore, the upper bainite evolved faster than the lower bainite region (Fig. 8).

Region I: Above the IT 670°C, the microstructures were a combination of austenite, ferrite, and pearlite

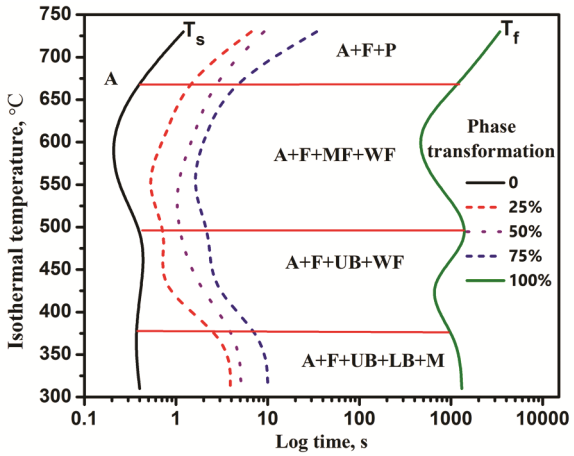

Fig. 8 — Time-temperature-transformation diagram of AISI 1010 steel.

product phases. This transformation was very close to the austenitizing condition.

Region II: IT 670°C - 470°C, the two different product phases were found as massive ferrite and widmanstätten ferrite while ferrite phase was the same as previous but no pearlite phase was formed in this region.

Region III: IT 500°C - 370°C, one more new phase evolved as bainite in which upper bainite was found in larger fraction, while other phases were observed in the same amounts as in the previous region II.

Region IV: Below IT 370°C, the region was the bainite region where the lower bainite phase dominated. However, fine WF and ferrite phases were also observed along the grain boundaries. A small amount of martensite was also traced in this region due to supercooling.

4 Conclusion

From the present study, the following conclusions have been drawn due to changes in isothermal temperatures that impacted on the microstructure of AISI 1010 steel:

(i) The austenitised microstructure of steel has been found to consist predominantly of ferrite and pearlite when it transforms into a combination of ferrite, pearlite, widmanstätten ferrite, massive ferrite, upper and lower bainite, and martensite, etc., at different isothermal holding temperatures.

(ii) Ferrite with pearlite has been observed at higher isothermal temperatures while bainite with martensite has been observed at lower isothermal temperatures.

(iii) C-curve nose has been observed clearly at 610°C where the incubation period required for transformation of austenite to product phases has been the smallest.

Acknowledgment

Thermo-mechanical simulator Gleeble®3800 has been procured from the FIST grant (SR/FST/ETI-216/2007 dated 06.02.2008) of DST New Delhi.

References

1 Rajput S K, Chaudhari G P, & Nath S K, *J Mater Process Tech*, 237 (2016) 113.
2 Sajjadi S A, & Zebarjad S M, *J Mater Process Tech*, 189 (2007) 107.
3 Qiu C, & Zwaag S V, *Steel Res Int*, 68 (1997) 32.
4 Tyagi R, Nath S K, & Ray S, *Metall Mater TransA*, 32 (2001) 359.
5 Calvo J, Rezaeian A, Cabrera J M, & Yue S, *Eng Fail Anal*, 14 (2007) 374.
6 Kerr H, *Int J Press Vessel Pip*, 4 (1976) 119.
7 Davenport E S, & Bain E C, *Trans AIME,* 90 (1930) 117.
8 Miodownik A P, & Saunders N, *Mater Sci Tech,* 18 (2002) 861.
9 Zhang B, Jiang Z, Li H, Zhang S, Feng H, & Li H, *Mater Charac,* 129 (2017) 31.
10 Kundu M, Ganguly S, Datta S, & Chattopadhyay P P, *Mater Manuf Process,* 24 (2009) 169.
11 Smuk O, *Microstructure and Properties of Modern P/M Super Duplex Stainless Steels*, Ph D Thesis, Royal Institute of Technology, Stockholm, 2004.
12 Kim Y, *Phase transformation in cast duplex stainless steels*, Ph D Thesis, Iowa State University, 2004.
13 Wan J, Ruan H, Wang J, & Shi S, *Mater Sci Eng A*, 711 (2018) 571.
14 Wang X F, Chen W Q, & Zheng H G, *Int J Miner Metall Mater*, 17 (2010) 435.
15 Kumar S, Nath S K, & Kumar V, *Metallogr Microstruct Anal*, 5 (2016) 264.
16 Singh S B, Mechanisms of bainite transformation in steels, in: Phase Transformations in Steels, ed. by Pereloma Elena and Edmonds David V, (Woodhead Publishing Series in Metals and Surface Engineering, Cambridge), 1st Edn, ISBN: 9780857096104, 2012, 385.
17 Mesplont C, *Phase Transformations and Microstructure - Mechanical Properties Relations in Complex Phase High Strength Steels*, Ph D Thesis, Ghent University, Belgium, 2002.
18 Machado I F, & Padilha A F, *ISIJ Int*, 40 (2000) 719.
19 Humphreys E S, Fletcher H A, Hutchins J D, Garratt-Reed A J, Reynolds W T, Aaronson H I, Purdy G R, & Smith G D W, *Metall Mater Trans A,* (2004) 1223.
20 Kumar S, Isothermal Transformation Behavior and Microstructural Evolution of Micro-Alloyed Steel, in: Eng. Steels High Entropy-Alloys, edited by Sharma A, Kumar S, Duriagina Z, (IntechOpen, London), 1st Edn, ISBN:978-1-83880-556-2, 2020, 27.